Proceedings of Symposium on Ultrasonic Electronics, Vol. 32 (2011) pp. 387-388
8-10 November, 2011

Performance Comparison of Optical Spectrometry and Stroboscopic Imaging for Size Distribution Measurement of Acoustic Cavitation

音響キャビテーション計測における光スペクトロメトリとストロボ撮影法の比較

Takanobu Kuroyama[1‡], Tadashi Ebihara[1], Koichi Mizutani[1], and Takeshi Ohbuchi[2] ([1]Univ. Tsukuba; [2]National Defense Academy;)
黒山 喬允[1‡], 海老原 格[1], 水谷 孝一[1], 大淵 武史[2] ([1]筑波大・システム情工, [2]防衛大・応物)

1. Introduction

High intensity ultrasound irradiated into water generates acoustic cavitation bubbles. The bubbles are attracting attentions and studied actively for its unique features.[1, 2] The diameter distribution of the bubbles is an important parameter. However, it is not easy to measure that because the small bubbles change their diameters with the frequency of the ultrasound. To measure the fluctuation of the diameter distribution, a measurement method using an optical spectrometer has been studied by the authors.[3] This method can measure the periodic fluctuation of the diameter distribution. In previous study, we indicated that the observational possibility of the bubbles using the method qualitatively. However, the result of the method was not validated quantitatively.

In this paper, volumetric (volume based) diameter distribution of acoustic cavitation bubbles is measured by optical spectrometry. The volumetric distribution also measured by stroboscopic imaging[4] to obtain the reference data. To validate the result of the optical spectrometer quantitatively, the results of the above two methods are compared.

2. Measurement principle and experiment

2.1 Experimental setup

Experimental setup is shown in **Fig. 1**. Ultrasound is irradiated by a bolt-clamped Langevin-type transducer (BLT). The ultrasound generates acoustic cavitation bubbles. The output plane of the BLT touches to surface of water in a glass cell. Size of the glass cell is 50 × 50 × 150 mm^3 and the water depth is 145 mm. The BLT is driven by cw sinusoidal voltage whose frequency is 46.2 kHz.

2.2 Optical spectrometer

In Fig. 1, an optical system along the z-axis is the optical spectrometer. Parallel light, whose vacuum wavelength λ is 632.8 nm, passes through a rectangular aperture of 10 × 1 mm^2, which defines the measurement area. The passing light irradiates the bubbles which distributes 3 mm below from the surface of the BLT. Outgoing light from the bubbles enters a Fourier transform lens whose focal length f is 500 mm. A photodetector measures the light intensity on the focal plane of the lens. The light intensity distribution on the focal plane is proportional to the spatial Fourier transformation (spatial spectrum) of the bubbles' projection along the light axis. Assuming that the bubbles are spherical and the spatial spectrum changes corresponding to the phase of the driving voltage of the BLT ϕ, the spatial spectrum $I(r, \phi)$ is shown as follows[3]:

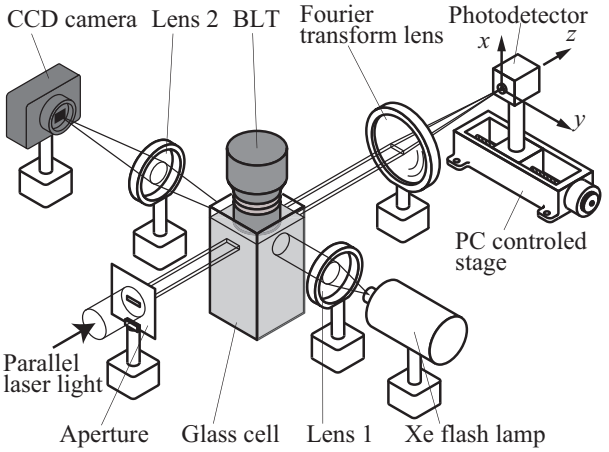

Fig. 1 Schematic diagram of measurement system.

$$I(r,\phi) = C\int_0^\infty s(a,\phi)\left(\frac{a}{2}\right)^4\left\{\frac{J_1[\pi ar/(\lambda f)]}{\pi ar/(\lambda f)}\right\}^2\frac{\pi a^3}{6}da, \quad (1)$$

$$r = \sqrt{x^2+y^2}, \quad (2)$$

where, C, a, J_1, and $s(a, \phi)$ are the proportionality coefficient, the diameter of the bubbles, the first-order Bessel function of the first-kind, and the proportion of the bubbles whose diameter is a at ϕ, respectively. In eq. (1), $\pi a^3/6$ means the volume of the bubble. Then, $s(a, \phi)$ expresses the volumetric diameter distribution of the bubbles. The photodetector is one dimensionally scanned from r = 3 to 50 mm along the y-axis by a personal computer (PC) controlled stage. The number of the measurement points is 50. The scanning pitch changes exponentially with r. The output signals of the photodetector are measured by a digitizer and transferred to the PC at the each point. The sampling frequency of the digitizer is 5 MHz. Then, the

mizutani@iit.tsukuba.ac.jp

phase resolution is about 0.06 rad. The output signals are 1×10^4 times averaged synchronously with the driving voltage of the BLT. The background light intensities are also measured and subtracted from the averaged waveforms. To reconstruct $I(r, \phi)$ from the averaged waveforms, the reconstructing method in Ref. 3 is applied.

The volumetric diameter distribution of the bubbles at ϕ is calculated by curve fitting. Assuming that $s(a, \phi)$ follows Rosin-Rammler type distribution which is used to express the size distribution of the bubbles and shown in eq.(3).[5] The parameters, $c(\phi)$, $n(\phi)$, and $b(\phi)$, are determined to minimize the square error between measured $I(r, \phi)$ and the spatial spectrum calculated from eq. (1) and eq. (3) by trust region reflective algorism[6].

$$s(a,\phi) = c(\phi)a^{n(\phi)-1}\exp(-b(\phi)a^{n(\phi)}). \quad (3)$$

2.3 Stroboscopic imaging system

In Fig. 1, an optical system along the direction of the y-axis is the stroboscopic imaging system. Lens 1 collimates pulsed light emitted from a Xe flash lamp. The duration of the light is 180 ns. The collimated light irradiates the bubbles. Lens 2 is focused to the bubbles crossing the parallel light of the optical spectrometer and forms the image of the bubbles on a CCD of a camera. Pulse timing of the light is synchronized to ϕ. The size of the captured image is 1280 × 720 px which corresponds to 1.18 × 0.667 mm^2. The images are captured 200 times at $\phi = 0, \pi/2, \pi$, and $3\pi/2$, respectively. Measurement by this method is performed just after that by the optical spectrometer.

The diameter distribution is determined by image analysis. The diameters of the bubbles are measured by detecting circular edges of the bubbles. The minimum detection diameter is set to 10 px (9.26 μm). Number diameter distribution n_i of diameter interval $[a_i \ a_{i+1})$ is determined by the detected diameters. The number diameter distribution is transformed to volumetric diameter distribution v_i by following equation:

$$v_i = \frac{n_i\left[(a_{i+1}+a_i)/2\right]^3}{\sum_{i=1}^{m} n_i\left[(a_{i+1}+a_i)/2\right]^3}, \quad (4)$$

where, a_1, $a_{i+1} - a_i$, and m, are 0 μm, 3 μm, and 26, respectively.

3. Results and Discussion

Measured fluctuation of volumetric mean diameter is shown in **Fig. 2**. The mean diameter changes in an acoustic cycle. At $\phi = \pi/2$, the mean diameters for the optical spectrometry and the stroboscopic imaging are different substantially. **Figure 3** shows the diameter distributions at $\phi = 0, \pi/2, \pi$, and $3\pi/2$. The bars show the volumetric diameter distribution measured by the stroboscopic imaging.

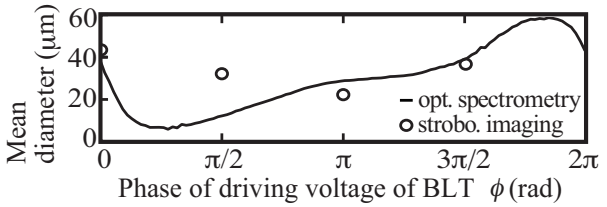

Fig. 2 One-cycle fluctuation of volumetric mean diameter of bubbles.

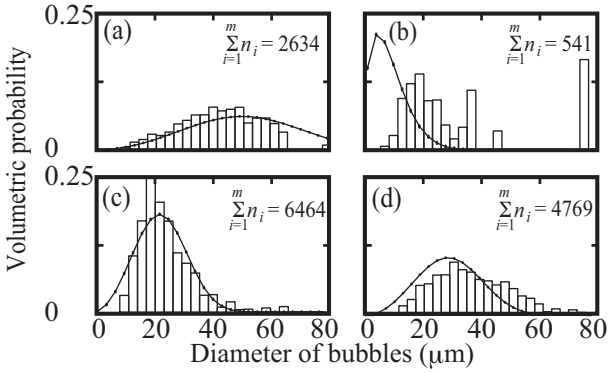

Fig. 3 Measured diameter distribution; (a)-(d): distributions for $\phi = 0, \pi/2, \pi$, and $3\pi/2$, respectively.

The solid lines show the volumetric diameter distribution measured by the optical spectrometry. The figure also shows the total number of the detected bubbles. The diameter distributions measured by the optical spectrometry are similar to those measured by the stroboscopic imaging at $\phi = 0$, π, and $3\pi/2$. However, at $\phi = \pi/2$, those differ substantially. It might be caused that the diameters of the bubbles are under the lower measurement limit of the stroboscopic imaging system, because the total number of the detected bubbles is significantly smaller than those of the others.

4. Conclusion

Volumetric diameter distribution of acoustic cavitation bubbles was measured by optical spectrometry. The result was compared to the reference data measured by stroboscopic imaging. As a result, it is indicated that the result of the optical spectrometer is similar to the reference data. Thus, the validity of the result of the optical spectrometer was confirmed.

References

1) R. Hosokawa, T. Saito, and H. Okawa: Jpn. J. Appl. Phys. **50** (2011) 07HE11.
2) Z. Zu, and K. Yasuda: Jpn. J. Appl. Phys. **50** (2011) 07HE07.
3) T. Kuroyama, T. Ebihara, K. Mizutani, T. Ohbuchi: Jpn. J. Appl. Phys. **50** (2011) 07HE05.
4) T. Kozuka, S. Hatanaka, T. Tuziuti, K. Yasui, and H. Mitome: Jpn. J. Appl. Phys. **39** (2000) 2967.
5) A. H. Englert, R. T. Rodoriques, and J. Rubio: Int. J. Miner. Process. **90** (2009) 27.
6) T. F. Coleman and Y. Li: Math. Program. **67** (1994) 189.